Studies of a scintillator-bar detector for a neutron wall at an external target facility*

YU Yu-Hong(余玉洪)[1,2;1)] XU Hua-Gen(徐华根)[1] XU Hu-Shan(徐瑚珊)[1;2)] ZHAN Wen-Long(詹文龙)[1]
SUN Zhi-Yu(孙志宇)[1] GUO Zhong-Yan(郭忠言)[1] HU Zheng-Guo(胡正国)[1] WANG Jian-Song(王建松)[1]
CHEN Jun-Ling(陈俊岭)[1] ZHENG Chuan(郑川)[1,2]

1 (Institute of Modern Physics, Chinese Academy of Sciences, Lanzhou 730000, China)
2 (Graduate University of Chinese Academy of Sciences, Beijing 100049, China)

Abstract To achieve a better time resolution of a scintillator-bar detector for a neutron wall at the external target facility of HIRFL-CSR, we have carried out a detailed study of the photomultiplier, the wrapping material and the coupling media. The timing properties of a scintillator-bar detector have been studied in detail with cosmic rays using a high and low level signal coincidence. A time resolution of 80 ps has been achieved in the center of the scintillator-bar detector.

Key words BC408, scintillator, time resolution, cosmic ray

PACS 29.30.Hs

1 Introduction

A combination of detectors for measuring neutrons, light charged particles, and efficient γ-rays is the trend in building powerful tools for nuclear physics research in recent years. Many neutron detector arrays have been employed to measure neutrons produced in nuclear reactions at energies from several tens of MeV/u to GeV/u, such as LAND at GSI[1] and MoNA at NSCL[2], and great progress has been made in understanding the nuclei far from the β stability line[3, 4] with those advanced detector systems. As a part of the project of the Cooling Storage Ring of the Heavy Ion Research Facility in Lanzhou (HIRFL-CSR), an External Target Facility (ETF), which is also a terminal of the second Radioactive Ion Beam Line in Lanzhou (RIBLL II), is under construction at the Institute of Modern Physics (IMP), CAS[5]. This facility will use both stable nuclei and radioactive ion beams (RIBs) to explore the structure of the exotic nucleus near the drip-line and the equation of state of asymmetric nuclear matter.

In Phase I of the ETF, a fast timing detector is located just in front of the reaction target to generate the reference signal for the time-of-flight measurements. A set of multiwire chambers and ionization chambers is used for particle identification and tracking before they hit the target. The target is surrounded by some high-purity germanium (HPGe) Clover detectors for on-line γ-ray coincidence measurements. A large acceptance dipole is placed 1 m downstream to the target to deflect the charged particles away from the axis, and there are several sets of position and timing detectors on both sides of the beam axis for tracking and identifying the charged particles.

The neutron wall, a key element of the ETF, is a high-efficiency, position-sensitive, multi-layer detector system for measuring neutrons of energies from several tens of MeV to $\sim$1 GeV. It is located in the beam axis and 14 m away from the target. The detector has 252 units in 14 layers, and the units are

Received 28 September 2008

* Supported by Knowledge Innovation Project of Chinese Academy of Sciences (CXTD-J2005-1, KJCX2-SW-N18), and NSFC (10635080, 10221003)

1) E-mail: yuyuhong@impcas.ac.cn

2) Corresponding author. E-mail: hushan@impcas.ac.cn; Tel.: +86-931-4969-325; Fax: +86-931-4969-329

parallel to each other in the same layer and perpendicular to the adjacent layers. A detailed description of this neutron wall can be found in Ref. [6]. In order to get high efficiency for low energy neutrons (<200 MeV), the first two layers of the detector (36 units) use a scintillator-only structure instead of the sampling structure used by others. This paper presents results of detailed studies done on those scintillator-bar detectors with cosmic rays.

2 Test setup

Figure 1(a) shows the layout of the test setup of a scintillator-bar detector with cosmic rays. The scintillator-bar, manufactured by Saint Gobain Corporation, is 144 cm long with a cross-section of 8 cm× 8 cm. It is made of BC408 scintillator material, with a decay time of 2.1 ns, a light attenuation length of 210 cm, a refractive index of 1.58 and a peak emission at 425 nm[7]. A 27 cm long light guide, which is shaped for better light collection according to the simulation, is glued to each end of the scintillator-bar with optical cement BC600 for light collection. The light generated in the scintillator-bar is read out by two inch photomultipliers (PMTs) from both ends of the bar.

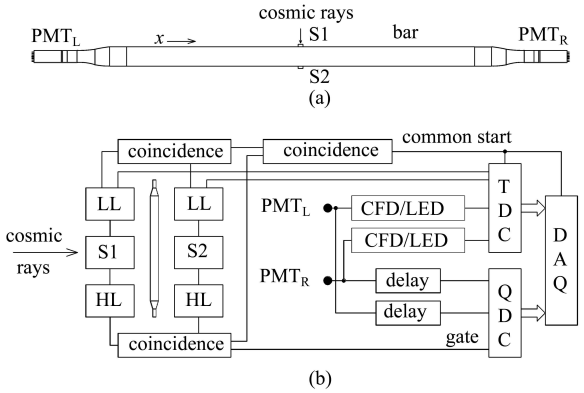

Fig. 1. (a) Experimental setup for scintillator bar-measurement, (b) Block diagram of the electronics.

S1 and S2, two small scintillators with dimensions 2 cm × 2 cm × 1 cm and 7.8 cm × 2.8 cm × 1 cm respectively, are used as the trigger detectors in the test. They are read out with PMT R7525 (Hamamatsu)[8], and a time resolution of about 80 ps can be achieved. These two detectors are mounted on a movable frame and measurements at 15 different points along the x axis have been carried out for the study ($x = 0$, ±5, ±15, ±25, $\cdots$, ±65 cm).

Figure 1(b) shows the block diagram of the electronics. To obtain a high quality trigger signal, a high level (HL) and a low level (LL) coincidence[9] have been used for S1 and S2. The signals from S1 or S2 are sent into two independent discriminators with different thresholds. The output signal from the discriminator with low level marks the arrival time of the detected events precisely, and the HL signal is used to reduce the occasion coincidence events. The generated signal with this double-level-coincidence is used as a common start of the TDC and provides a trigger to the Data AcQuisition system (DAQ). The PMT signal from each end of the scintillator-bar is split linearly into two. The PAW[10] is used for data analysis.

3 Results and discussion

For a neutron detector, used in neutron energy measurement by the time-of-flight method, the timing resolution and efficiency will be the most important parameters. In order to get the best results, detailed studies on the PMT choice, the wrapping material, and the coupling medium between different materials have been carried out.

3.1 PMT and PMT base

As the read-out device, a high gain, fast time response, good linearity and long-term stability are the necessary requirements for a PMT to measure the weak fluorescence resulting from the secondary particle produced by neutron reactions.

Different tubes from Hamamatsu, EMI and other companies were tested. Silica oil was used to couple the tubes to the scintillator bar, which was wrapped in aluminum foil, and the output signals were processed by a Constant Fraction Discriminator (CFD) CF583 for the time information.

After considering the different factors, we chose R7724, which was specially designed by Hamamatsu for our purpose, as the read-out device. The time resolution was evaluated by the standard deviation of the time difference σ between the two ends of the bar, and the light yield was obtained by integrating the signal of the PMT with QDC for each end. We defined $Q_g = \sqrt{Q_L Q_R}$, and this is related to the number of photos produced by the incident particle. Table 1 shows the comparison between it and XP2020, a very popularly used one. From the results, we can see that R7724 has almost the same performance as XP2020, and a much lower working voltage and cost.

Parameters of the Hamamatsu R7724 PMT.

minimum effective area	ϕ 46 mm
typical voltage	1800 V
anode pulse rise time	<2.0 ns
transit time spread	1.1 ns
wavelength of maximum response	420 nm
number of stages	10
typical gain	1.8×10^7
quantum efficiency at 420nm	26%

Table 1. Results measured with different PMTs.

phototube	Q_g/pC	σ_{CF583}/ps
XP2020	$380\pm^{34}_{19}$	154±6
R7724	$387\pm^{35}_{19}$	155±6

To get the best time resolution while keeping a wide linear dynamic range, the voltage divider circuit of the PMT was modified from the manufacturer's model. It complements the tube characteristics by maintaining good pulse fidelity through a wide range of signal currents and sustain high count rates. A circuit diagram of the base is shown in Fig. 2. The voltage across the middle stage dynodes is the same, while the first dynode is quintupled to ensure high electron collection efficiency. The last three dynodes with decoupling capacitors maintain good linearity as well as large pulses. The three damping resistors alleviate the output signal oscillations. The signal from the anode is picked off for both timing and energy measurements.

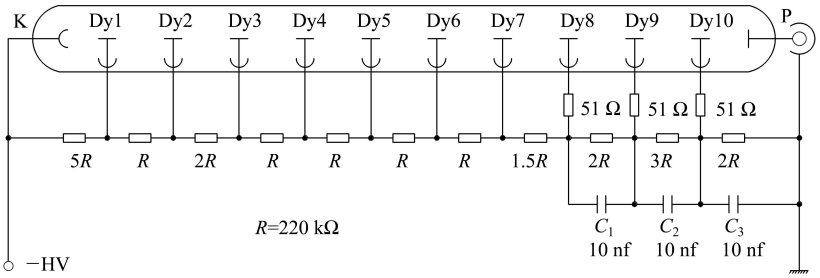

Fig. 2. Circuit diagram of the phototube base.

3.2 Wrapping material

The material used for bar wrapping plays an important role in the light reflection, which influences the light collection and leads to different time resolution. An investigation is necessary for choosing a good wrapping material which can greatly improve the timing performance of the detector.

Table 2. Performances of different Tyvek products.

Tyvek type	thickness/mm	Q_g/pC	σ_{CF583}/ps
1082D	0.26	$364\pm^{31}_{18}$	218±8
1073D	0.21	$420\pm^{37}_{21}$	168±7
1056D	0.15	$401\pm^{36}_{20}$	168±7
1025D	0.13	$377\pm^{34}_{19}$	175±7

Five different wrapping materials were studied with all the other conditions remaining the same: the original wrapping (coming with the scintillator from Saint Gobain), aluminum foil, Teflon tape, aluminized Mylar foil and Tyvek 1056D[11]. The light was shielded with black plastic tapes in all cases to reduce the noise and cross-talk. Here we chose Tyvek 1056D from many other Tyvek products by considering all the requirements, such as timing resolution, light collection efficiency, mechanical property and so on. Table 2 shows the property of 1056D comparison with other Tyvek products.

Five points were measured along the bar with a distance of 24 cm between the adjacent points for each case in the test. The result is shown in Fig. 3, and Tyvek 1056D is better than any others both in time resolution and the number of photon collected. Fig. 3 also indicates the optimal timing resolutions obtained for interactions at the center of the bar, despite a lower photon collection probability. Other reports also show that the wrapping material will affect the time resolution[12, 13], and that aluminium foil is better than Tyvek. We consider that different types of Tyvek may be used in the study.

3.3 Coupling medium

A good coupling medium can reduce light loss when photons go through the interfaces between the scintillator-bar, the light guide and the PMT entrance window. At the same time, some degree of mechanical flexibility would compensate for length variations of the detector due to manufacturing tolerances and temperature effects. To achieve the maximum light

output, easy assembly and maintenance, the light guides were glued to the bar with the optical cement BC600. Usually, silicon cement is a good choice. Considering long-term stability and maintenance, it is found that silicon cement would become dry and is not very suitable for our case. Instead, EJ560, a silicon cushion produced by ELJEN Company[14], was selected as the interface coupling medium to avoid a rigid coupling of light guides to the PMT windows. Care was taken to reduce the gas bubbles between the optical interfaces when using the cushion.

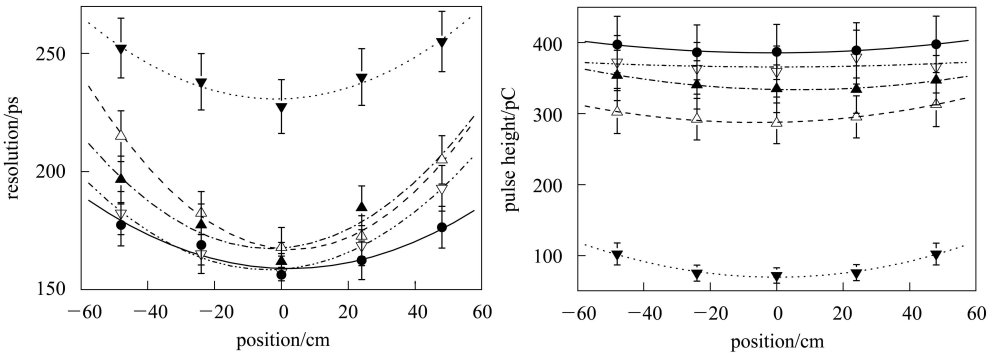

Fig. 3. σ $(T_{\rm L}-T_{\rm R})$ and $Q_{\rm g}$ obtained from five different wrapping materials shielded with black plastic: (1) solid uptriangle (▲) aluminum foil, (2) solid downtriangle (▼) original wrapping, (3) open uptriangle (△) Teflon, (4) open downtriangle (▽) aluminized Mylar foil, (5) solid circle (●) Tyvek 1056D. The curves are added to guide the eye.

3.4 Timing performance

From the test, the average time obtained from the left (right) side of the bar at each measurement position is proportional to the distance of the position to the PMT, and the slope of the line represents the effective speed of light along the bar with a value of 17.2 cm/ns. The average light emittance angle of the light is 24.5°, calculated with $\cos(\theta_{\rm eff})=\dfrac{v_{\rm eff}}{c/n}$. Here c is the velocity of light in the vacuum and n is the refractive index of the material.

For a thicker scintillator-bar detector, the Moyal fit[15] gives a really good description of the pulse height distribution with each point of the QDC spectrum well fitted. If the geometric deformation of the detector module is ignored, the scintillation light propagation in the bar will obey $N(x)=N_0{\rm e}^{-x/\lambda}$, where N_0 and N are the number of the photons at the hit point and distance x, respectively, and λ is the attenuation length of the bar. The value of the attenuation length can be deduced from $\dfrac{1}{\lambda}=-\ln\left(\dfrac{N}{N_0}\right)\dfrac{1}{x}$. The QDC peak value corresponding to the position x is shown in Fig. 4 and the attenuation length is deduced to be 106 cm. It is smaller than the value provided by the manufacturer, and also smaller than the value we get from the average light emittance angle, which is about 190 cm. This means a lot of photons emitted in a large angle have also been collected due to reflection on the scintillator-bar surface wrapped with the Tyvek product.

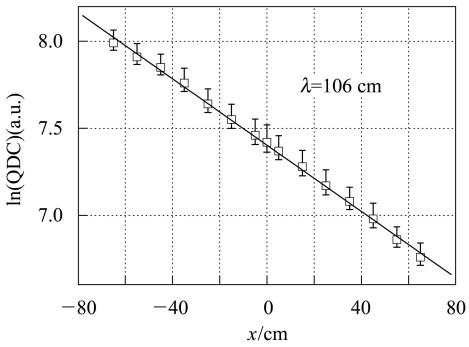

Fig. 4. Natural log of average pulse height versus x. The asymmetric error bar shows that a high-energy long tail exists in the pulse height distribution caused by high-energy δ-rays, as cosmic rays pass through an 8 cm thick scintillator-bar.

Because the bar is read out from both ends, each event will be measured twice independently. Defining $T_{\rm L}$ ($T_{\rm R}$) as the time interval of the PMT signal from the left (right) end of the bar relative to the common start of TDC, the weighted mean time, $T_{\rm av}$, can be calculated according to the formula[16],

$$T_{\rm av}=\frac{T_{\rm L}\sigma^2(T_{\rm R})+T_{\rm R}\sigma^2(T_{\rm L})}{\sigma^2(T_{\rm L})+\sigma^2(T_{\rm R})} \quad (1)$$

and the time resolution can be extracted from

$$\frac{1}{\sigma^2(T_{\rm av})}=\frac{1}{\sigma^2(T_{\rm L})}+\frac{1}{\sigma^2(T_{\rm R})}\,, \quad (2)$$

where σ ($T_{\rm L}$) and σ ($T_{\rm R}$) are the resolution for the measurements at the left and right ends of the bar, and the errors from TDC start time and the electronics have already been subtracted.

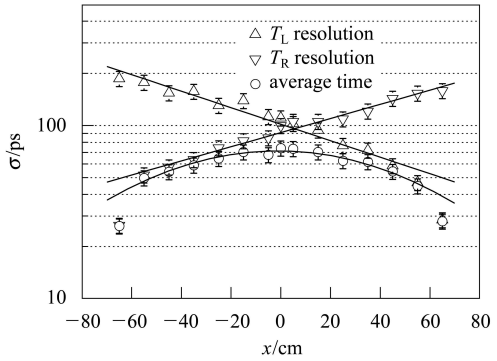

Fig. 5. Time resolutions of σ ($T_{\rm L}$), σ ($T_{\rm R}$) and σ ($T_{\rm av}$) versus x. The curves are shown to guide the eye.

Figure 5 shows the time resolution as a function of the position of the measurement points. The time resolution σ ($T_{\rm av}$) of the scintillator-bar is less than 80 ps when the cosmic rays penetrate through the central area, and even better around the two ends. The reason for the poorer time resolution obtained in the center is due to the small attenuation length, and fewer photons collected at both ends.

4 Summary

The timing performance of the scintillator-bar detector of a neutron wall has been studied with cosmic rays. The PMT and PMT base, the wrapping material and the coupling medium have been studied in detail to achieve the required time resolution. A special PMT, R7724, has been developed by Hamamatsu Corporation and a timing-type base is adopted to obtain a better time resolution. The wrapping material also plays an important role in improving the time resolution and Tyvek has demonstrated its superiority over others. An optimum coupling medium provides a better timing performance as well as easy maintenance. A time resolution of 80 ps can be reached in the center of the scintillator-bar detector.

References

1 BLaich T H et al. Nucl. Instrum. Methods A, 1992, **314**: 136
2 Karch L, Bohm A, Brinkmann K Th et al. Nucl. Instrum. Methods A, 2001, **460**: 362
3 Aumann T. Nucl. Phys. A, 2005, **752**: 289c
4 Jonson B. Nucl. Phys. A, 2004, **734**: 263
5 XIA J W, ZHAN W L, WEI B W et al. Nucl. Instrum. Methods A, 2002, **488**: 11
6 XU Hua-Gen, XU Hu-Shan, LI Wen-Fei et al. HEP & NP, 2006, **30**: 57 (in Chinese)
7 http://www.bicron.com
8 http://www.hamamatsu.com
9 Kichimi H, Yoshimura Y, Browder T et al. Nucl. Instrum. Methods A, 2000, **453**: 315
10 http://paw.web.cern.ch/paw/
11 http://www.MedicalPacking.dupont.com
12 Kim Y D et al. Nucl. Instrum. Methods A, 1996, **372**: 435
13 WANG Feng-Mei et al. HEP & NP, 2006, **30**: 776 (in Chinese)
14 http://www.apace-science.com/eljen/ei-560.htm
15 Moyal J. Philos. Mag., 1955, **46**: 263
16 Denisov S, Dzierba A, Heinz R et al. Nucl. Instrum. Methods A, 2002, **478**: 440